

# Dielectric Characterization of Fog in the Terahertz Regime

A. ETINGER<sup>a</sup>, Y. GOLOVACHEV<sup>a</sup>, G.A. PINHASI<sup>b</sup> AND Y. PINHASI<sup>a,\*</sup>

<sup>a</sup>Dept. of Electrical and Electronic Engineering, Ariel University, P.O. Box 3, Ariel 40700, Israel

<sup>b</sup>Dept. of Chemical Engineering, Ariel University, P.O. Box 3, Ariel 40700, Israel

Electromagnetic radiation at millimeter and sub-millimeter (terahertz) wavelengths are being considered for various applications, including remote sensing, wireless communications, and radars. However, wireless links implemented in millimeter wavelengths above 30 GHz suffer from absorption and dispersion effects in air, which emerge mainly due to oxygen molecules, humidity, and water droplets. Such frequency dependent atmospheric propagation effects become more severe as the frequency is increased to the terahertz regime. Moreover, weather conditions like haze, fog, and rain cause a further decrease in the overall link-budget leading to a degradation in the channel performance. In the current paper, the physical properties of the atmosphere and their effect on the electromagnetic radiation within the sub-millimeter wavelengths are studied theoretically and experimentally. Expressions for the attenuation and group delay are presented in terms of the electric susceptibility of the atmospheric medium in the presence of suspended water droplets. The analytical estimations are demonstrated experimentally in a controlled water fog chamber.

DOI: [10.12693/APhysPolA.136.749](https://doi.org/10.12693/APhysPolA.136.749)

PACS/topics: 41.20.Jb, 84.40.-x, 92.60.Ta

## 1. Introduction

The growing demand for broadband wireless communication links and the deficiency of wide frequency bands within the conventional spectrum, require utilization of higher microwave and millimeter-wave spectrum at the extremely high frequencies (EHF) above 30 GHz [1]. In addition to the fact that the EHF band (30–300 GHz) covers a wide range, which is relatively free of spectrum users, it offers many advantages for wireless communication and radar systems.

When millimeter-wave radiation passes through the atmosphere, it suffers from frequency-dependent absorptive and dispersive phenomena, causing distortions in amplitude and phase. Several empirical and analytical models were suggested for estimating the millimeter and infrared wave transmission of the atmospheric medium [2, 3].

Models are used to study the effect of clouds and fog on the electromagnetic signal, in particular the attenuation and time delay [4–6]. Recently, experimental study in ultra-low visibility artificial fog in a confined space was performed using an artificial fog produced by a “smoke machine” [7]. It was found that apart from the attenuation, the incremental group delay caused by the fog also played a role in the accuracy of the radar as was analyzed theoretically in [5].

In the present work, the effect of suspended water droplets was studied theoretically and experimentally to find the effect of the foggy conditions on the signal strength and time delay. In the theoretical part of the study, analytic expressions of dielectric medium parameters like permittivity, refractivity, and susceptibility, and the relation between them are presented.

Using the derived expressions a modified millimeter-wave propagation model (MPM) is employed for the prediction of the suspended water droplets effect. In the present experimental part of the study, a dense water-fog chamber was used to demonstrate the effects for frequency-modulated continuous wave (FMCW) radar, experimentally. The results were compared to the analytical model predictions.

## 2. Propagation in dielectric media

Propagation of electromagnetic waves in the open space is affected by various factors that cause distortion in the amplitude and phase. In general, such effects are due to refraction, absorption, and dispersion due to the dielectric properties of gases composing air. The MPM is used to predict the atmospheric frequency response [4].

These effects are described by the propagation expression for the field in the frequency domain. Propagating a distance  $d$  in a homogeneous, linear medium, the resulted field is proportional to

$$\tilde{E}_{\text{out}}(f) \propto \tilde{E}_{\text{in}}(f) e^{-jk(f)d}, \quad (1)$$

where  $\tilde{E}_{\text{in}}(f)$  and  $\tilde{E}_{\text{out}}(f)$  are the transmitted and received fields respectively, presented as phasors in the frequency domain. The parameter  $k(f)$  is a frequency dependent *propagation factor*:

$$k(f) = 2\pi f \sqrt{\mu_0 \varepsilon(f)}, \quad (2)$$

where  $\varepsilon(f)$  is the *electric permittivity* and  $\mu_0$  is the magnetic permeability of vacuum. The electric permittivity depends on the dielectric properties of the medium and can be written as

$$\varepsilon(f) = \varepsilon_r(f) \varepsilon_0 = \underbrace{[1 + \chi_e(f)]}_{\varepsilon_r(f)} \varepsilon_0, \quad (3)$$

\*corresponding author; e-mail: [yosip@ariel.ac.il](mailto:yosip@ariel.ac.il)

using the *electric susceptibility*  $\chi_e(f) = \chi'_e(f) - j\chi''_e(f)$ , which is a complex, frequency dependent quantity. The vacuum permittivity is  $\varepsilon$  and  $\varepsilon_r(f) = \varepsilon'(f) - j\varepsilon''(f)$  is the complex *relative permittivity*, for which

$$\varepsilon'(f) = 1 + \chi'_e(f), \quad \varepsilon''(f) = \chi''_e(f). \quad (4)$$

Introducing Eq. (3) and (4) into (1) results in

$$k(f) = \frac{2\pi f}{c} \sqrt{\varepsilon_r(f)} = \frac{2\pi f}{c} \underbrace{\sqrt{1 + \chi'_e(f) - j\chi''_e(f)}}_{n(f)}, \quad (5)$$

where  $c = 1/\sqrt{\mu_0\varepsilon_0} \approx 2.997 \times 10^8$  m/s is the speed of light in vacuum. We identify the *refractive index*  $n(f) = \sqrt{1 + \chi'_e(f) - j\chi''_e(f)}$ . Since the electric susceptibility of the air is  $|\chi_e(f)| \ll 1$ , one can use the approximation  $\sqrt{1+x} \approx 1+x/2$  and express the refraction index via the complex electric susceptibility as

$$n(f) \cong 1 + \underbrace{\frac{1}{2}\chi'_e(f) - j\frac{1}{2}\chi''_e(f)}_{N(f) \times 10^{-6}} \quad (6)$$

The MPM model [4] defines the *refractivity*  $N(f) = N_0 + N'(f) - jN''(f)$  in parts per million (ppm). It contains a real nondispersive part  $N_0$ , and a real  $N'(f)$  and imaginary  $N''(f)$  frequency dependent terms. These are related to the electric susceptibility as follows:

$$\begin{aligned} [N_0 + N'(f)] \times 10^{-6} &= \frac{1}{2}\chi'_e(f), \\ N''(f) \times 10^{-6} &= \frac{1}{2}\chi''_e(f). \end{aligned} \quad (7)$$

During the propagation of the millimeter wave signals in the atmospheric medium, absorption and phase dispersion occur. Following Eq. (5) and approximation (6), the propagation factor  $k(f) = -j\alpha(f) + \beta(f)$  can now be expressed in terms of the attenuation coefficient

$$\alpha(f) = -\text{Im}(k(f)) = \frac{\pi f}{c} \chi''_e(f) \quad (8)$$

and the wave number

$$\beta(f) = \text{Re}(k(f)) = \frac{2\pi f}{c} \left[ 1 + \frac{1}{2}\chi'_e(f) \right]. \quad (9)$$

Propagating a distance,  $d$ , the time delay in the atmosphere is

$$\tau_d(f) = \frac{d}{2\pi} \frac{d\beta}{df} = \underbrace{\frac{d}{c}}_{\tau_0} + \underbrace{\frac{d}{2c} \frac{d}{df} [f\chi'_e(f)]}_{\Delta\tau_d(f)}, \quad (10)$$

where we define time delay in vacuum as  $\tau_0 = d/c$ . Additional group delay is caused by the atmosphere due to its electric dispersive susceptibility  $\chi'_e(f)$ :

$$\Delta\tau_d(f) = \frac{d}{2c} \frac{d}{df} [f\chi'_e(f)] = \frac{\tau_0}{2} \left[ \chi'_e(f) + f \frac{d\chi'_e(f)}{df} \right]. \quad (11)$$

The presented model was incorporated in the MPM and used for calculation of the atmospheric frequency response various conditions. Contributions of dry air, water vapor, suspended water droplets (haze, fog, cloud), and rain are addressed.

In the current work, emphasis is given to the study of foggy atmospheric conditions with the presence of suspended water-droplets in air. The suspended water-droplet susceptibility term is derived from the Mie scattering theory using the Rayleigh approximation, which applies for the case when the scattering particle is small relative to the wavelength (i.e., size parameter  $x = 2\pi R_p/\lambda \ll 1$ ). In the case of particles with dimensions greater than the wavelength, ( $x > 1$ ) Mie's scattering model should be used.

Using the Rayleigh approximation, the model provides both amplitude and phase information independent of the particle size distribution. The susceptibility was found to be proportional to the suspended water droplet concentration  $W$ , in g/m<sup>3</sup>. The real  $\chi'_e(f)$  and imaginary  $\chi''_e(f)$  parts of the electric susceptibility are [3]:

$$\begin{aligned} \chi'_e(f) &= 3W \left( 1 - \frac{3}{\varepsilon_0 + 2} \right) + 9W \left( \frac{1}{\varepsilon_0 + 2} - \frac{\eta/\varepsilon''_W}{1 + \eta^2} \right), \\ \chi''_e(f) &= 9W \frac{1}{\varepsilon''_W (1 + \eta^2)}, \end{aligned} \quad (12)$$

where  $\varepsilon'_W$  and  $\varepsilon''_W$  are the real and imaginary parts of the dielectric permittivity of the suspended water (in distinction to the permittivity of the medium,  $\varepsilon(f)$  as in (3)), and  $\eta(f) = [2 + \varepsilon'_W(f)]/\varepsilon''_W(f)$ . The quantities in detail can be found in [2, 3, 6].

### 3. The fog chamber setup

The effect of suspended water droplets on a radar signal at the higher band of the millimeter waves, 330 GHz, was studied experimentally. A set of experiments were conducted for various visibility conditions (visibility down to 0.5 m). The results were used to validate the model for tested conditions.

The experimental setup is based on a high-resolution FMCW radar system placed in a confined indoor space filled with water fog. The radar system and a metal target were placed in two far ends of closed space. The chamber shown in Fig. 1a has a dimension of  $18 \times 2.5 \times 2$  m<sup>3</sup>, where the distance between the radar and the target was  $d = 18$  m. The space was filled with water fog created by a set of four ultrasonic foggers (piezoelectric transducer fog machine) as shown in Fig. 1b. The spatial fog spread in space was homogenized using a series of small fans along the chamber.

The FMCW radar system (see Fig. 2) contains an oscillator and antenna and a pair of horn-lens antennas. The HP-8350B frequency-sweeping synthesizer is employed as a primary driver of the local oscillator (LO). Its frequency was tuned to sweep from 10 to 10.31 GHz and multiplied by a factor 32 providing linear FM signal starting from  $f_0 = 320$  GHz with a sweep of  $BW = 10$  GHz. The sweep time was set to be  $T_s = 9.6$  ms. The transmitted power was 10 dBm. Both the transmitting and receiving antennas were ELVA-1 custom design Gaussian horn-lens antenna with a gain of 40 dBi and linear horizontal polarization [8].



Fig. 1. (a) The fog chamber and (b) the fog streaming machine.



Fig. 2. The J-Band millimeter wave radar.

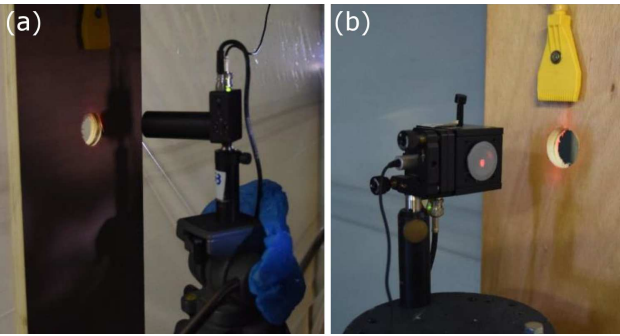


Fig. 3. Red laser light system for visibility measurement: (a) Laser transmitter, (b) Photo detector.

The detected signal obtained at the output of the harmonic mixer at the receiver chain was analyzed using a spectrum analyzer, model R&S FSV40. The radar-detected signal was measured in both cases with and without fog and its spectrum was analyzed to find the corresponding intermediate frequency (IF), which is the result of the overall group delay  $\tau_d$  along the path [5]. Following [7], the relation between the incremental part  $\Delta\tau_d$  of the time delay given in (11) can be measured via the frequency shift  $\Delta f_{IF}$  in the resulting intermediate frequency according to

$$\Delta\tau_d = \frac{T_s}{BW} \Delta f_{IF}. \quad (13)$$

Within the confined space, the thermodynamics properties as the temperature, barometric pressure, and relative humidity were measured. The visibility was estimated using pairs of laser transmitter and photodetector

at a wavelength of 632 nm as shown in Fig. 3. The laser and detector units were placed in several places along the chamber to evaluate the fog uniformity. The droplet size distribution was also measured by a laser diffraction technique using the Spraytec of Malvern Instrument.

Fog and clouds contain visible cloud water droplets or ice crystals suspended in air. They are normally formed at a relative humidity (RH) near 100%. The fog is characterized often with parameters like visibility  $Vis$  [m], droplet number concentration  $n_d$  [ $\text{cm}^{-3}$ ], and mass liquid water content  $W$  [ $\text{g}/\text{m}^3$ ]. In the current study the Gultepe relation between these three parameters was adopted [9]:

$$Vis = 1002 (n_d W)^{-0.6473}. \quad (14)$$

#### 4. Results and discussion

The effect of fog on an FMCW radar signal at carrier frequency 330 GHz ( $\lambda = 0.09$  mm) was studied experimentally and the results were compared with the model predictions. The experiments with the radar were performed without fog, as a background case, and with fog for various visibility values.

The initial thermal conditions in the test space were 16°C and 80% RH. The typical droplet size in fog is 10  $\mu\text{m}$ . This leads to size parameter ( $x = 2\pi R_p/\lambda < 1$ ) corresponding to the Rayleigh approximation for the scattering model.

The output IF signal was recorded in the frequency domain. The signal obtained contained relatively large fluctuations, mainly due to multi reflections from different objects along the experimental chamber. After numerical smoothing the spectra for various visibility values are presented in Fig. 4. From the difference between the measured peaks of the spectra with and without fog, one can identify the attenuation and frequency shifts summarized in Table I.

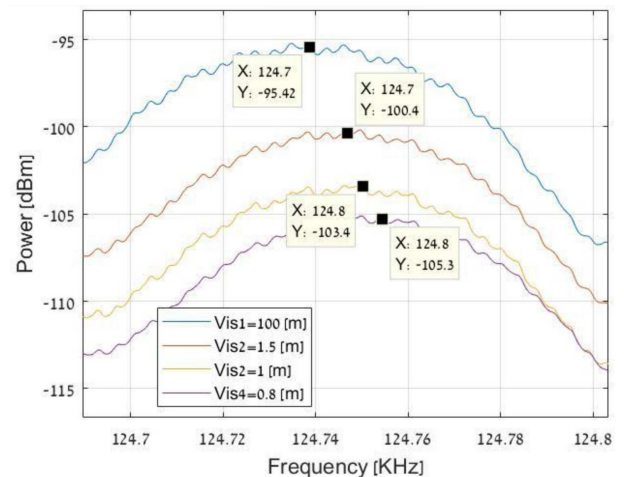


Fig. 4. The spectra of the radar intermediate frequency for various visibility conditions.

TABLE I

Comparison between measured and calculated results with 330 GHz radar (exp. — experimental, calc. — calculated).

Visibility Vis [m]	Liquid water content $W$ [g/cm <sup>3</sup> ]	Fog attenuation factor $\alpha$ [dB/km]		Intermediate frequency shift $\Delta f_{IF}$ [Hz]	Incremental part of the time delay $\Delta\tau_d$ [ps/km]	
		exp.	calc.		exp.	calc.
0.8	24	361	430	16	427	345
1	17	277	311	12	320	323
1.5	9	222	174	10	267	290
100	0.01	0	0	0	0	0

The modified MPM was used to predict the fog effect. For the model input, the water liquid content,  $W$ , was estimated using liquid fog relations (14). For the water content evaluation in the very low visibility conditions, the droplet number concentration values,  $n_d$ , were estimated for to be around 2500 cm<sup>-3</sup>. A good agreement was found between the experimental results and the theoretical predictions with respect to attenuation and time delay for very low visibility values.

### 5. Summary and conclusions

In the current work, the absorptive and dispersive characteristics of the atmosphere containing suspended water droplets as in foggy conditions were studied theoretically and experimentally. In the theoretical part an analysis of the attenuation and group delay that emerged due to the suspension of water droplets in the atmosphere was presented. The dielectric properties of the atmospheric medium in terms of the electric susceptibility was derived.

The measurements were done in a special fog chamber, using high-resolution FMCW radar operating at 330 GHz. The high bandwidth of the radar and its extended frequency sweep allow revealing the effects quantitatively. The experimental measurements showed an agreement with the calculated results predicted by the theory.

### Acknowledgments

We would like to thank Dr. Ayala Ronen and Dr. Ofir Shoshanim from the Israel Institute for Biological Research for their help in conducting the experiments in the fog chamber.

### References

- [1] W. Feng, Y. Li, D. Jin, L. Su, S. Chen, *Sensors* **16**, 892 (2016).
- [2] H.J. Liebe, *Int. J. Infrared Millim. Waves* **10**, 631 (1989).
- [3] ITU-R P.840-6, *International Telecommunication Union*, Geneva 2013.
- [4] Y. Pinhasi, A. Yahalom, G.A. Pinhasi, *J. Opt. Soc. Am. B* **26**, 2404 (2009).
- [5] N. Balal, G.A. Pinhasi, Y. Pinhasi, *Sensors* **16**, 1 (2016).
- [6] Y. Golovachev, A. Etinger, G.A. Pinhasi, Y. Pinhasi, in: *J. Applied Physics* **125**, 151612 (2019).
- [7] Y. Golovachev, A. Etinger, G.A. Pinhasi, Y. Pinhasi, *Sensors* **18**, 2148 (2018).
- [8] B. Kapilevich, Y. Pinhasi, R. Arusi, M. Anisimov, D. Hardon, B. Litvak, Y. Wool, *J. Infrared Millim. Terahertz Wave* **31**, 1370 (2010).
- [9] I. Gultepe, M.D. Muller, Z.A. Boybeyi, *J. Appl. Meteorol. Climatol.* **45**, 1469 (2006).